A Framework for Real-Time Power Management of a Grid-Tied Microgrid to Extend Battery Lifetime and Reduce Cost of Energy

S.A. Pourmousavi, *Student Member, IEEE,* Ratnesh K. Sharma, Babak Asghari, *Student Member, IEEE*

***Abstract*— Because of different technical and economical concerns, battery is happened to be an inevitable part of a microgrid as well as the most expensive component. This fact brings up the necessity of a real-time power management to guarantee the maximum possible battery lifetime based on the final cost of energy. In this way, this study attempts to present a real-time management framework for a grid-tied microgrid based on battery life and cost estimation. In order to verify the effectiveness of the proposed framework, a grid-tied commercial microgrid, which is equipped with wind turbine, PV solar panels and Li-Ion battery package, is optimally sized by HOMER® and dynamic models of different components have been developed in MATLAB/Simulink®. Then, simulation study has been carried out for a year on the system. All data such as load demand, wind, temperature, solar radiation, and time-based electricity tariff are grasped from different places for a year. Results show that the proposed framework effectively extends the battery lifetime while slightly decreases the cost of energy for customer.**

***Index Terms*—Li-Ion battery, grid-tied microgrid, real-time power management.**

I. Nomenclature

L_R	Battery cycle life at rated DoD and discharge current.
D_R	DoD for which rated cycle life was determined.
C_R	Rated ampere-hour capacity at rated discharge.
u_0, u_1, and u_2	Coefficients of the DoD fitting function.
D	Actual DoD.
C_A	Actual capacity at discharge current.
d_{act}	Ampere-hour of the discharge event.
T	System operation time, day.
AC	Annualized Cost, $/year.
RBC	Rated Battery Capacity, kW.
CC	Capital Cost, $/kW.
RC	Replacement Cost, $/kW.
SFF	Sinking Fund Factor.
CRF	Capital Recovery Factor.
O&MC	Annual Operation and Maintenance Cost, $/kAh/year.
f	Inflation rate, %.
i	Actual interest rate.
i_{nom}	Nominal interest rate, %.
NO. rep	Number of Replacement of the battery, round (Y_{proj} / Y_{rep}).
Y_{proj}	Useful lifetime of the project, year.
Y_{rep}	Useful lifetime of the battery calculated by BLE, year.
P_W	Wind power, kW.
P_{PV}	PV solar power, kW.
P_{grid}	Scheduled power from the grid, kW.
P_{load}	Load demand, kW.
SoC	State of Charge of the battery, %.

S.A. Pourmousavi (e-mail: s.pourmousavikani@msu.montana.edu), is with the Electrical and Computer Engineering Department, Montana State University, Bozeman, MT 59717 USA (currently with NEC labs America as intern), Ratnesh K. Sharma (e-mail: ratnesh@sv.nec-labs.com), and Babak Asghari (e-mail: babak@sv.nec-labs.com) are with NEC Laboratories America, Cupertino CA 95014 USA.

II. Introduction

Microgrid is an emerging technology which promises to achieve many simultaneous goals for power system stakeholders, from generator to consumer [1]. Its framework offers a mean to capitalize on diverse energy sources in a decentralized way, while reducing the burden on the grid by generating power close to the consumer. Since microgrid with distributed generation (DG) systems fall within city load centers (<69 kVA) at electric utility substations, near feeders, within neighborhoods, and at industrial, commercial, and residential customer locations [2], storage devices such as battery are necessary to:

- Manage electric grid peak demand
- Improve reliability and outage mitigation, compensate for intermittent power generation from DGs
- Provide ancillary services specifically in islanded mode of operation
- Increase electric grid load factor and utilization via the smart grid.

As a result, storage devices are immediate components of microgrids as a mean to achieve high penetration of

978-1-4577-2159-5/12/$31.00 ©2011 IEEE

intermittent renewable energy resources into the grid. According to [2], the desired size of the energy storage device for distributed energy storage systems (DESS) application is 25-200 kW 1-phase and 25-75 kW 3-phase while its duration and desired lifetime are 2-4 hours and 10-15 years, respectively. The desired values in the case of commercial and industrial (C&I) energy management are 50-1000 kW in size, 3-4 hours duration, and 15 years lifetime [2]. Based on these facts, different battery technologies, such as Lithium-Ion batteries, can be promising candidate for these applications.

The available power from renewable energy components, particularly wind turbine, is highly variable and somewhat random. Consequently, batteries in hybrid power systems, whether in DESS or C&I energy management applications, experience a very irregular pattern of charge and discharge cycles. On the other hand, it is well-known that battery life depends on discharge pattern. Therefore, managing discharge pattern is a promising approach to battery life maximization. Since one can say that maximum battery lifetime can be achieved (i.e. the nominated lifetime) when it always kept idle, there should be a rational definition for maximum lifetime of the battery. In this research, this term is defined as the maximum possible battery lifetime by taking the cost of energy in to consideration at each time step of management. In other words, the maximum battery lifetime is beneficial as long as the cost of the energy provided for the customer is minimum at the time of management.

While most research has been focused on optimal sizing and unit commitment of such systems [3], few deal with real-time management of a hybrid energy system [3]. To the best knowledge of the authors, none have addressed the same concern in the management problem. This paper attempts to introduce a management framework to achieve maximum battery lifetime based on battery life estimation and the price of energy. The proposed procedure is developed for the grid-tied microgrids which include wind turbine and PV solar panels as generation assets and Li-Ion battery as storage device. The system is optimally designed using HOMER® with real wind speed, solar radiation, grid electricity price, and load demand data. Since unit commitment problem is beyond the scope of this study, the scheduled grid power in real-time simulation is taken to be the same as the output grid power from HOMER®. Then, dynamic model of each component for the designed system is developed in MATLAB/Simulink®. Various power management strategies are then implemented on the dynamic model of the microgrid with actual data for a year. Eventually, results are compared.

Rest of the paper is organized as follows: In Section III, the proposed power management framework is discussed. Then, the battery life estimator (BLE) is presented in Section IV. Section V is devoted to mathematical formulation of the cost of energy from battery (CEB). Finally, simulation results for different part of the proposed framework are shown in Section VI, followed by the conclusion in Section VII.

III. Proposed Real-time Power Management Framework

Batteries are usually equipped with battery management system (BMS) which is defined as any electronic device that manages a rechargeable battery (cell or battery pack), by monitoring its state, calculating secondary data, reporting that data, protecting it, controlling its environment, and/or balancing it. However, there is no real-time supervisory power management system on the top level of microgrid to regulate battery discharge in order to maximize its lifetime. While battery is usually the most expensive part of such systems at the time of installation, and needs frequent replacement despite other components, a real-time power management seems tremendously helpful to guarantee the appropriate use of battery. Generally, real-time management strategy performs at a smaller time interval, e.g., every few seconds or minute. Results of such systems are the power share between different generation and storage assets.

In one hand, real-time management operates on existing system with certain amount of DG resources and storage devices. On the other hand, it is well known that power from PV and wind is almost free after installation because of no fuel cost. Thus, it is beneficial to capture all available power from wind and PV. Therefore, the real-time management problem is reduced to power sharing between battery and grid. Grid power is available from the grid at time-of-use rates, and is limited to a maximum of 40kW. The reason could be a weak distribution system, lack of enough generation, and/or low capacity of different equipements such as overhead lines and/or transformer. As mentioned earlier, the purchased power from the grid is scheduled a day ahead as unit commitment problem. In this study, the authors are not dealing with the unit commitment problem. Therefore, the scheduled power from the grid is considered as a known input parameter in to the management system. The battery will be charged only in the case of excess power from PV and wind. In other words, battery will not be charged by the power purchased from the grid.

Replacement cost is the most effective factor in the CEB calculation. Based on the discharge pattern, batteries need to be replaced periodically to maintain system performance. Therefore, it can be concluded that the CEB depends on battery aging which directly depends on discharge pattern. As a result, the power management should decide upon the discharge pattern and the associated lifetime and cost. Since maximum possible life of the battery occurs when battery is kept idle (which is not reasonable), there should be a competing objective. Final cost of energy is considered as the competing objective in this paper. The general schematic block-diagram of the energy management unit (EMU) with different components of grid-tied system is shown in Fig. 1. In order to calculate the cost of energy from the battery, it is anticipated to calculate the number of its replacements during the lifetime of the project. As a result, it is required to estimate the battery lifetime based on the discharge pattern up to the point of management. Therefore, the management strategy

starts with the battery lifetime estimation, which is shown as Battery Life Estimator (BLE) unit, Fig. 1. Consequently, the CEB will be estimated, in $/kWh. Eventually, the decisions will be made based on the defined secondary management (SM) strategy between battery and grid. Any scenario, such as the ones defined in this study or heuristic optimization, can be defined as SM block for battery discharging.

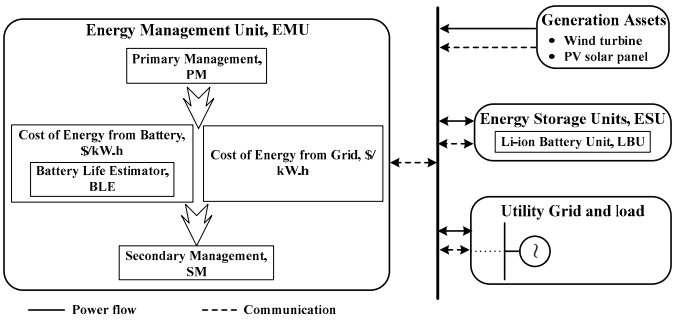

Fig. 1. Schematic diagram of the management framework.

Since the overall management system is responsible for both charging and discharging of the battery, the proposed framework is broken into two hierarchical steps as follows:

- *Primary Management (PM)*: In this step, primary decisions about power flow between generation resources and the energy storage unit will be made based the information from different generation assets, battery state of charge (SOC) and availability of the grid. This part of the management is shown in Fig. 2.
- *Secondary Management (SM)*: Whenever discharging battery or purchasing extra power from the grid is required, the decision will be made by the proposed scenarios in order to extend the battery lifetime based on the final price of energy for the customers.

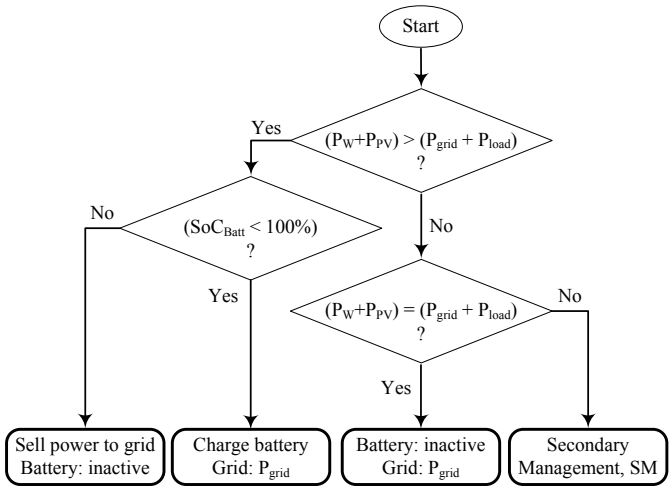

Fig. 2. PM schematic diagram.

IV. Battery Life Estimator, BLE

In this section, the applied BLE technique is described in details. Different techniques in literatures are developed for battery life estimation; however most of them show at least one of the following critical shortcomings for the purpose of this study:

- Complicated, slow, and time consuming techniques [4], [7]
- Requiring detailed information about battery performance which is not usually available in battery datasheets [5], [6], [8], [9], [10], and [11]
- Large estimation intervals, with significant error [7], [10]
- Valid for a certain type of batteries [5], [6]

In this study, a battery life prediction technique which is introduced in [12] and [13] is used. This technique is based on the three premises which have been developed in [14]. Varying depths of discharge and varying rates of discharge are considered as two primary determinants of battery life in this technique. Assuming the presence of environmental controls, temperature-based battery aging can be ignored. A significant feature of this technique is that it bases its analysis on battery performance and cycle life data provided by the manufacturer, supplemented by a limited amount of empirical test data. The present battery lifetime estimator also eliminates the need for an electrochemical model of the battery [12]. The principle ideas of this technique are introduced in the following premises:

Premise 1: Each cell has a finite life [12]. It will reach the end of its useful life when the cumulative effective ampere-hours of individual effective ampere-hours corresponding to a series of discharge events equal the rated charge life of the cell. The rated charge life is given as [12]:

$$\Gamma_R = L_R . D_R . C_R \tag{1}$$

Premise 2: The actual charge life of the cell is a function of the DoD. Therefore, the effective ampere-hour discharge in a given discharge event may be more or less than the actual discharge based on the actual DoD. In order to determine this functional relationship, the following function has been used to perform the best fit to the cell cycle life data vs. DoD [12]:

$$L = u_2 \left(\frac{D_R}{D} \right)^{u_0} . \boldsymbol{exp} \left(u_1 \left(1 - \frac{D}{D_R} \right) \right) \tag{2}$$

Different methods can be applied to perform the curve fitting. Two different methods have been used in this study including particle swarm optimization (PSO) [3] and non-linear least square (NLLS) method from MATLAB curve fitting toolbox. It is shown in [3] that PSO, as a heuristic optimization technique, is able to achieve optimal solution in a small fraction of a second. Also, NLLS is a popular regression method which has been used in [12] and [13]. The results of curve fitting are shown in simulation results.

Premise 3: The charge life of the cell, Γ, drops whenever the cell is discharged at a rate faster (higher discharge current) than the rated rate. Furthermore, the reduction in life will have a close functional relationship to the observed reduction in ampere-hour capacity with increasing discharge rate [12]. This effect can be expressed fairly accurately by the following two-parameter function:

$$d_{eff} = \left(\frac{C_R}{C_A}\right)^{v_0} .\exp\left(v_1\left(1-\frac{C_R}{C_A}\right)\right).d_{act} \quad (3)$$

Since battery manufacturers typically conduct battery life testing at a single discharge rate, usually the rate for which the cell's rated capacity is given, enough data is not available to determine the parameters v_0 and v_1. Therefore, the effect of discharge rate will be estimated using a simplified form of Eq. (3) where v_0 is set equal to 1 and v_1 is set to 0:

$$d_{eff} = \left(\frac{C_R}{C_A}\right).d_{act} \quad (4)$$

In order to calculate C_A related to each discharge event, 1-D cubic spline interpolation has been applied in this study. Using (2) and (4), the effects of DoD and discharge rate are combined simply by multiplying the factors as follows [12]:

$$d_{eff} = \left(\frac{D_A}{D_R}\right)^{u_0} .\exp\left(u_1\left(1-\frac{D_A}{D_R}\right)\right).\left(\frac{C_R}{C_A}\right).d_{act} \quad (5)$$

Eq. (5) gives the effective discharge for a single discharge event. In order to estimate the lifetime of a battery which has been exposed to a series of discharge patterns, accumulative effective discharge is required. Finally, lifetime of the battery can be calculated as follows [12]:

$$L_{time} = \frac{L_R.D_R.C_R}{\sum_{i=1}^{n} d_{eff,i}}.T \quad (6)$$

The procedure of battery life estimation is shown in Fig. 3.

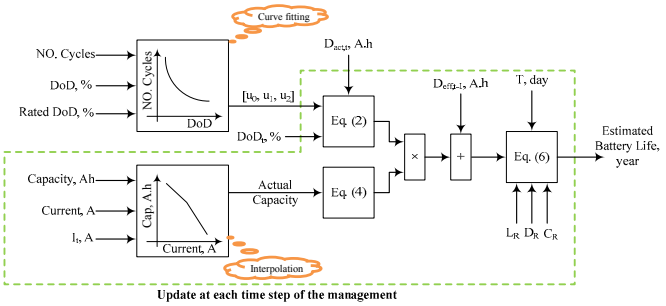

Fig. 3. BLE model in a single block-diagram.

V. Cost of Energy from Battery (CEB) Calculation

The number of battery replacements over the lifetime of the project can be calculated from the estimated battery life. In this study, the following cost model is used to calculate the CEB [15] and [16]. Note that the cost of charging the battery is zero is assumed to be free.

$$AC = RBC\times\left\{\left[CC + RC\times SFF\left(i,Y_{rep}\right)\right]\times CRF\left(i,Y_{proj}\right)\right\} + RBC\times O\&MC\times\left(1+f\right)^{n} \quad (7)$$

Where,

$$SFF\left(i,Y_{rep}\right) = \sum_{n=1}^{NO.rep} \frac{1}{\left(1+i\right)^{n\times Y_{rep}}} \quad (8)$$

$$CRF\left(i,Y_{proj}\right) = \left(i\times\left(1+i\right)^{Y_{proj}}\right) / \left(\left(1+i\right)^{Y_{proj}} - 1\right) \quad (9)$$

$$i = \left(i_{nom} - f\right) / \left(1+f\right) \quad (10)$$

The capital cost and O&MC of the battery are derived from [2] and [16], respectively. The capital cost of battery is dependent on its application [2]. For commercial building application in the range of 25-50 kWh, it is $4240/kW in average (the actual price varies from $2800 to $5600 /kW) [2]. Since the capital cost includes cost of battery, power electronics, cost of installation, step-up transformer, smart-grid communication and controls, and grid interconnection to utility, the replacement cost is considered to be 60% of the capital cost [2]. For O&MC, the given value in [16] is used which is equal to $50 /kAh/year. Additionally, the nominal annual interest and inflation rates are assumed to be 3.5% and 1.5%, respectively. In order to compare the cost of electricity from battery with that from grid, the cost of battery is translated to $/kWh instead of $/year. Thus, the cost of electricity from battery is expressed as follows:

$$CEB = AC / \left(8760\times RBC\right) \quad [\$/kWh] \quad (11)$$

VI. Simulation Results

In this section, simulation results for different parts of the proposed management framework are presented and discussed.

A. Results of curve fitting and interpolation

In this study, the Intensium Flex High Energy Lithium-Ion battery pack from SAFT company [17] is considered as storage device. The cycle life of the battery is plotted against DoD of the battery package in Fig. 4.

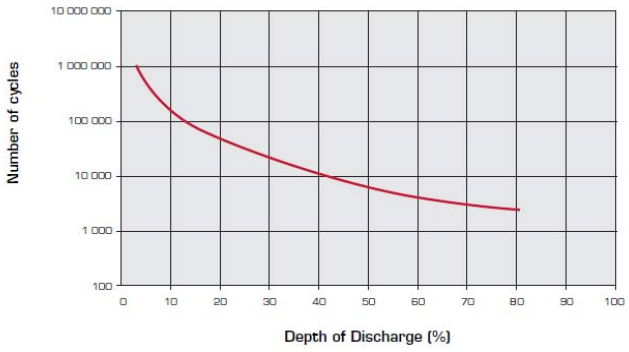

Fig. 4. Cycle life vs. DoD for Intensium Flex High Energy Li-Ion battery, SAFT Company.

Capacity at actual discharge current of interest is determined using the amperes in discharge tables commonly included in battery specification. Table I shows actual discharge current for different discharge time duration for the battery used in this study.

Table I: Amperes on Discharge table for Intensium Flex High Energy Li-Ion battery, SAFT company.

	Duration (min)					
Rated Capacity	1	10	30	60	180	300
45 A.h	197.92	131.25	75	40.62	14.17	9

As mentioned in Section IV, curve fitting on the data provided in Fig. 4 is required to determine the coefficients of the function in Eq. (2).Fig. 5 shows the curve fitting results using PSO and NLLS.

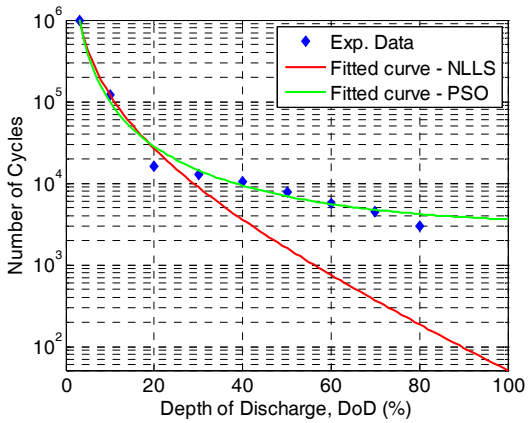

Fig. 5. Curve fitting results for two different methods.

The root mean square error (RMSE) of the curve fitting is 0.124 and 3.509 for PSO and NLLS methods, respectively. This error is defined as follows:

$$RMSE = \sqrt{\frac{x_1^2 + x_2^2 + \cdots + x_n^2}{n}} \qquad (12)$$

Where x_n is the error between data sample n and the value obtained by fitted curve. It can be concluded from Fig. 5 and the RMSE that the results from PSO are far better than the results from NLLS method. As a result of using PSO, battery lifetime estimation will be more accurate which results in a more accurate calculation for the cost of battery.

As discussed earlier, the value of discharge current has significant effect on battery aging. This impact is evaluated in Eq. (4) which requires data interpolation at certain discharge current using the given table from manufacturer (see Table I). Results of interpolation for Table I and a sample interpolated discharge current are shown in Fig. 6. As expected, the capacity of the battery diminishes when the discharge current increases. Based on theory, this effect nonlinearly increases for higher discharge current, shown in Fig. 6.

B. BLE and CEB test

Unfortunately, there was no experimental data available for battery discharge profile (current and duration) to test the BLE. Therefore, an arbitrary discharge profile is generated based on current and duration for a day which is reported in Table II. The discharge pattern is repeated for 100 days. The goal is to show the impact of curve fitting algorithm on battery life estimation and consequently the associated cost. It is assumed that the primary management keeps the battery in full SoC, thus enough power is always available to discharge.

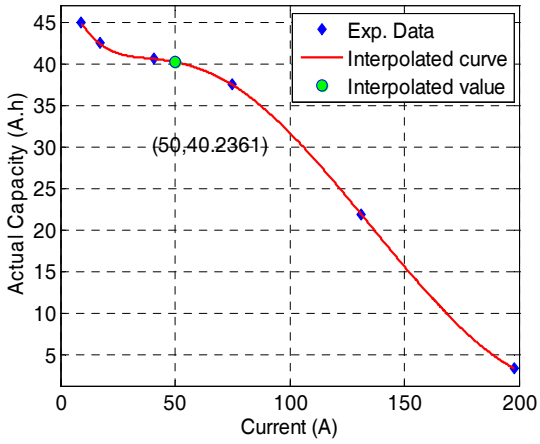

Fig. 6. Actual capacity of the battery at different discharge currents.

Total discharge time of the battery during a day is 165 minutes which is less than 3 hours a day. Different high power and energy pulses are considered in this pattern. Also, the discharge current is always kept below the critical value reported in Table II.

Table II: The discharge pattern for a day.

Time, min	1	1	1	2	2	3	4	4	5
Current, A	100	150	130	120	110	30	40	40	50
Time, min	5	5	10	11	11	20	20	30	30
Current, A	90	80	60	20	50	60	70	50	65

The BLE has been performed for different ratios of current and time duration in Table II, and each experiment has been carried out for NLLS and PSO. In Fig. 7, results obtained from both NLLS and PSO are shown when the discharge current is scaled from 90% to 130% of the values in Table II, while the time duration is constant. It can be seen from Fig. 7 that the estimated values from NLLS and PSO follow the same trend. However, the estimated values are significantly different at each point. In other words, error in BLE using NLLS approach can easily lead the CEB calculation to significant error.

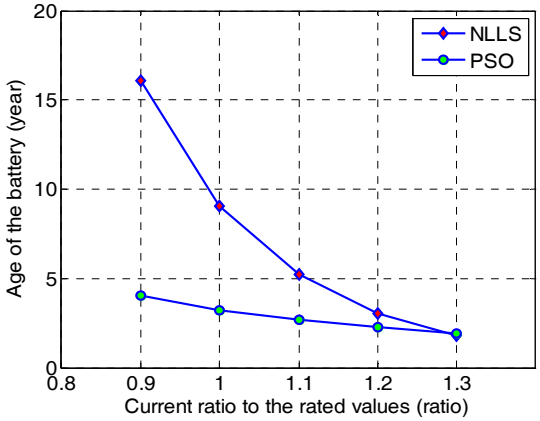

Fig. 7. Battery life estimation for different currents, obtained from the curve fitting with NLLS and PSO.

For the discharge pattern reported in Table II, the associated cost of the electricity from battery is calculated for both curve

fitting tools used in this study, NLLS and PSO. The useful lifetime of the project is considered to be 20 years. The battery cell has rated capacity of 45 Ah at 48 V as nominal voltage. The rated DoD is 80% based on the information provided by the company [17].

Fig. 8 shows the CEB for different ratio of discharge currents. Since the estimated battery lifetime in the case of PSO method is lower than those from NLLS method (Fig. 7), calculated cost of the energy from battery will be higher for PSO in comparison with NLLS method.

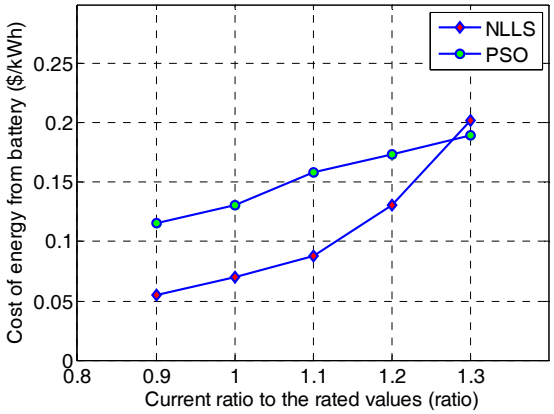

Fig. 8. CEB for different discharge currents, obtained from the curve fitting with NLLS and PSO.

Also, another simulation study has been performed on the proposed BLE model. In this case, the current is kept constant and the time duration of each discharge has been changed from 80% to 120%. Both NLLS and PSO have been applied for curve fitting. Results are shown in Fig. 9.

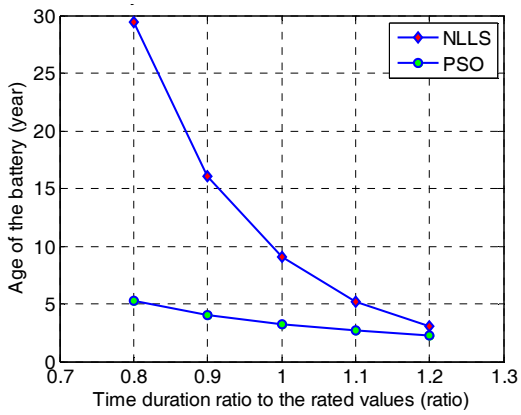

Fig. 9. Battery life estimation with different time duration, obtained from the curve fitting with NLLS and PSO.

The same observation can be made in this case as well. Since NLLS method presents significant error in curve fitting, it will result in a significant error in the battery life estimation which can be seen in Fig. 9.

In Fig. 10, the CEB is shown when discharge current is constant and the time duration of discharge pattern changes. It can be seen that the estimated CEB in the case of PSO are higher than the ones from NLLS for the same reason.

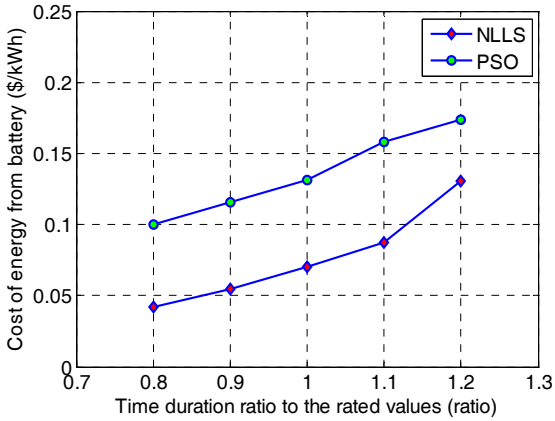

Fig. 10. CEB for different discharge time duration, obtained from the curve fitting with NLLS and PSO.

C. The proposed management framework

In order to test the proposed management framework and its effectiveness, a grid-tied microgrid includes wind turbine and PV solar panels as generation resources and Lithium-Ion battery pack as storage device is applied. The microgrid has been optimally sized with HOMER® considering the fact that the battery is not allowed to be charged by the grid. Also, the power purchased from the grid in the output of the HOMER® is used as scheduled hourly power from grid. Basically, this has to happen based on unit commitment problem at the beginning of each day for the day ahead. Since unit commitment methods work only in hourly basis with predicted load demand and renewable power generation, there is always a power mismatch in real-time operation of the system operation. Real-time power management is the only solution to avoid power mismatch and keep the system stable. The size of the system is as follows:

- ✓ Wind turbine: 20 kW
- ✓ PV solar panels: 40 kW
- ✓ Lithium-Ion battery: 38.8 kWh

The battery specification is given in Table III. Also, the system configuration can be seen in Fig. 1. Wind speed, PV solar radiation, temperature, and load demand data are actual minute-by-minute data. The load demand is grasped from a commercial building. The average load demand during a year, the peak load and load factor are 34.7 kW, 63.8 kW, and 0.546, respectively. For real-time power management, the dynamic model of each component has been developed in MATLAB/Simulink including all power electronic interfaces and controllers.

Table III: Intensium Flex High Energy Lithium-Ion battery specification.

Nominal voltage of each pack, V	48
Capacity (C/3), Ah	45
Lifetime at +20 °C perm, year	20
Lifetime at +40 °C, year	>10
Cycle life (80% DoD, 20 °C)	3000
NO. of pack in series, and parallel	6, and 1

Also, time-based electricity tariffs are considered in this study as reported in Table IV.

Table IV: Cost of electricity from grid.

Peak Summer[1]	$0.16489 /kWh
Part-Peak Summer[2]	$0.06595 /kWh
Off-Peak Summer[3]	$0.03298 /kWh
Part-Peak Winter[4]	$0.05334 /kWh
Off-Peak Winter[5]	$0.03556 /kWh

[1] 12:00 noon to 6:00 p.m. Monday through Friday (except holidays)
[2] (8:30 a.m. to 12:00 noon) AND (6:00 p.m. to 9:30 p.m.) Monday through Friday (except holidays)
[3] 9:30 p.m. to 8:30 a.m. Monday through Friday AND All day Saturday, Sunday, and holidays
[4] 8:30 a.m. to 9:30 p.m. Monday through Friday (except holidays)
[5] 9:30 p.m. to 8:30 a.m. Monday through Friday (except holidays) AND All day Saturday, Sunday, and holidays

As SM strategy in the proposed framework, three different scenarios are introduced in this study. The decisions from management framework are updated every minute to determine the share of power between battery and the grid. The simulation has been carried out for a year for each scenario.

CASE I. If the SoC of the battery is greater than 20% (since the rated DoD of the battery is 80% [17]), the battery should certainly provide the required power. Otherwise, the grid will provide the required power.

CASE II. If the SoC of the battery is greater than 20% and the CEB is less than the cost of energy from the grid, battery should meet the demand. Otherwise, the grid will provide the required power.

CASE III. In this case, it is assumed that there is no way to discharge the battery. Therefore, required power will be purchased from the grid no matter what its cost is.

Different other scenarios can be defined as SM such as heuristic optimization-based methodologies. For each case, simulation with the same data has been performed for a year and the results are shown in the following. Note that in CASE III, the battery has not been used. Therefore, the CEB and its lifetime is not important anymore and are not shown in results.

In Fig. 11, the battery life estimation for CASEs I and II is shown. In CASE I, the battery ages faster due to the more frequent usage. Therefore, it is expected to see a higher CEB in CASE I compared to CASE II, which can be seen in Fig. 12. At the beginning of the estimation, rapid variations can be observed due to lack of enough discharge information for estimation. However, the estimation is gradually converging along the time of the simulation.

In Fig. 11, it can be seen that the estimated battery lifetime in CASE II is varying quickly. These variations are the result of the battery life estimation which is very close to 20 years. Whenever the battery life estimation drops below 20 years, replacement cost for at least one battery will be added to the energy cost resulting in the variations shown in Fig. 12.

The accumulative CEB based on the battery usage for CASES I and II are shown in Fig. 13. Due to the increase of the battery life in CASE II, the cost of energy is reduced in this case which eventually results in a lower cost for the consumer.

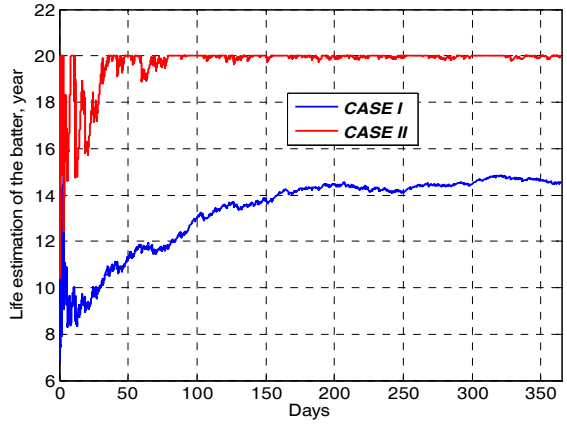

Fig. 11. Battery life estimation for CASES I and II for a year.

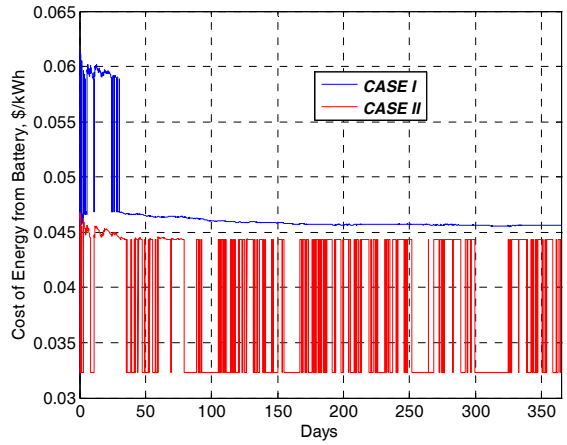

Fig. 12. CEB per kWh for a year.

Note that in both CASES, total load demand has been met either by the power from battery or the grid. However, the aggregated payment by the end of the year in CASE I is almost twice of the payment in CASE II. These results show the effectiveness of the proposed management framework in extending the battery lifetime and reducing the cost of energy for the consumer.

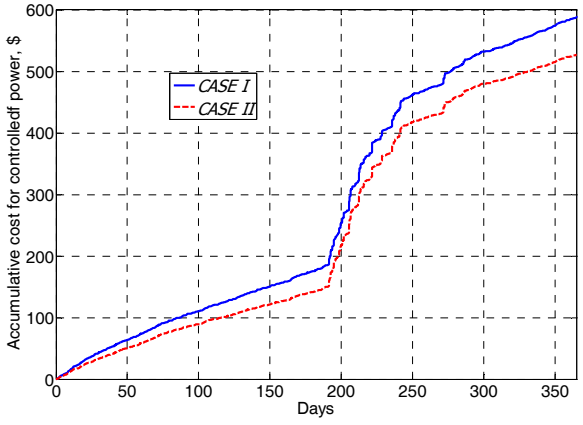

Fig. 13. Accumulative cost of controlled power during the year.

The total electricity payments for the controlled power at the end of the year for different CASES are presented in Table V. Respect to the controlled power final payment in CASE III,

a percentage of money has been saved in CASES I and II which are presented in Table V. In other words, it can be observed that the proposed management framework for CASES I and II, offers money saving at the end of the year. Also, the total payment (for controlled and uncontrolled power) at the end of the year has been improved 0.42% and 0.85% for CASE I and CASE II, respectively respect to CASE III. Due to relatively small size of the battery compared to other components in the microgrid, a small amount of load can be met by the battery, and the grid has the biggest share in providing power to the load. Therefore, the percentage of money saving is not significant. For a system with a larger battery, this percentage could increase remarkably.

Table V: controlled power cost in each case and percentage of savings.

	Battery payment, $	% of money saving
CASE I	588	9.26
CASE II	527	18.67
CASE III	648	--

VII. Conclusion

Storage devices are an integral part of any microgrid, technically and economically. Also, batteries are always known as the most expensive part of microgrids. In this study, a power management framework is proposed for a grid-tied microgrid with battery as storage device. The goal of the proposed management framework is extending the battery life and reducing the cost of the energy for the consumer. Simulation results show that both goals have been achieved through the proposed power management framework within three different scenarios.

References

[1] C.M. Colson, M.H. Nehrir, S.A. Pourmousavi, "Towards Real-Time Microgrid Power Management Using Computational Intelligence Methods," *Proceedings,* IEEE PES General Meeting, pp. 1-8, 2010.

[2] EPRI, "Electricity Energy Storage Technology Options: A White Paper Primer on Applications, Costs and Benefits," Dec, 2010. Web Address: http://www.electricitystorage.org/images/uploads/docs/EPRI_StorageReport_5_11.pdf

[3] S.A. Pourmousavi, M.H. Nehrir, C.M. Colson, C. Wang, "Real-Time Energy Management of a Stand-Alone Hybrid Wind-Microturbine Energy System Using Particle Swarm Optimization," *IEEE Trans. on Sustainable Energy*, vol. 1, Issue. 3, pp. 193-201, 2010.

[4] R. Hobbs, R. Newnham, D. Karner, "Fleming, F.; Development of Predictive Techniques for Determination of Remaining Life for Lead Acid Batteries Under Fast Ccharge," *In Proceeding*, Battery Conference on Applications and Advances, pp. 177-188, 1999.

[5] K. Takei, K. Kumai, Y. Kobayashi, H. Miyashiro, N. Terada, T. Iwahori, T. Tanaka, "Cycle Life Estimation of Lithium Secondary Battery by Extrapolation Method and Accelerated Aging Test," Journal of Power Sources, vol. 97-98, pp. 697-701, July 2001.

[6] A. Yamashita, H. Wakaki, K. Saito, T. Shodai, "Capacity Estimation and Lifetime Expectancy of Large-Scale Nickel Metal Hydride Backup Batteries," *In Proceeding*, Telecommunications Conference INTELEC, pp. 291-295, 2005.

[7] P.E. Pascoe, A.H. Anbuky, "Standby Power System VRLA Battery Reserve Life Estimation Scheme," *IEEE Trans. on Energy Conversion*, vol. 20, Issue. 4, pp. 887-895, 2005.

[8] C.C. Hua, T.Y. Tasi, C.W. Chuang, W.B. Shr, "Design and Implementation of a Residual Capacity Estimator for Lead-Acid Batteries," *In Proceeding*, Industrial Electronics and Applications, ICIEA, pp. 2018-2023, 2007.

[9] X. Wei, B. Zhu, W. Xu, "Internal Resistance Identification in Vehicle Power Lithium-ion Battery and Application in Lifetime Estimation," *In Proceeding*, International Conference on Measuring Technology and Mechatronics Automation, vol. 3, pp. 388-392, 2009.

[10] W.L. Burgess, "Valve Regulated Lead Acid Battery Float Service Life Estimation Using a Kalman Filter," *Journal of Power Sources*, vol. 191, Issue. 1, pp. 16-21, 2009.

[11] D. Haifeng, W. Xuezhe, S. Zechang, "A New SOH Prediction Concept for the Power Lithium-Ion Battery Used on HEVs," *In Proceeding*, IEEE Conference on Vehicle Power and Propulsion, VPPCEE, pp. 1649-1653, 2009.

[12] S. Drouilhet, B.L. Johnson, "A Battery Life Prediction Method for Hybrid Power Applications," AIAA Aerospace Sciences Meeting and Exhibit, 1997.

[13] J.F. Manwell, J.G. McGowan, U. Abdulwahid, K. Wu, "Improvements to the Hybrid2 Battery Model," Windpower 2005 Conference.

[14] P. Symons, "Life Estimation of Lead-acid Battery Cells for Utility Energy Storage," *In Proceeding*, 5th Conference on Batteries for Utility Storage, San Juan, Puerto Rico, July 1995.

[15] A. Kashefi Kaviani, G.H. Riahy, SH.M. Kouhsari, "Optimal Design of a Reliable Hydrogen-Based Stand-Alone Wind/PV Generating System Considering Component Outages," Renewable Energy, Vol. 34, Issue 11, Nov. 2009, pp: 2380-2390.

[16] H. Yang, W. Zhou, L. Lu, Zh. Fang, "Optimal Sizing Method for Stand-Alone Hybrid Solar/Wind System with LPSP Technology by Using Genetic Algorithm," Solar Energy, Vol. 82, Issue 4, April 2008, pp: 354-367.

[17] SAFT Batteries, Website: "http://www.saftbatteries.com/doc/Documents/stationary/Cube782/IntFLEX_0708.ce3d756b-b571-4cf3-a952-ad069f830ed1.pdf"

Biographies

S. Ali Pourmousavi (S'07) received the B.S. degree from University of Mazandaran, Iran in 2005 and M.S. degree from Amirkabir University of Technology (Tehran Polytechnic), Iran in 2008, all in electrical engineering. He is a Ph.D. student in the Electrical and Computer Engineering (ECE) Department at Montana State University. His research interests include energy management of hybrid generation system with DGs and storage, load control and demand response (DR), and wind speed and power forecasting.

Ratnesh K. Sharma (M'11) leads the Energy Management Department at NEC Laboratories America. He has a PhD degree from University of Colorado at Boulder and BTech. (Hons.) degree from Indian Institute of Technology, Kharagpur. His research interests span sustainable energy management in electricity, buildings and transportation sectors including energy conversion, power systems, communications and analytics. He has authored more than 135 papers/technical reports and holds 50 US patents.

Babak Asghari (S'06) received his Ph.D. degree from the University of Alberta, Canada. Currently, he is a researcher in the Energy Management Department at NEC Laboratories America. His research interests include real-time simulation and control of power systems and electrical drives.